ICARUS 116, 359–375 (1995)

A Search for Jupiter-Mass Companions to Nearby Stars

GORDON A. H. WALKER[1] AND ANDREW R. WALKER

Geophysics and Astronomy Department, University of British Columbia, Vancouver, British Columbia V6T 1Z4, Canada
E-mail: walker@astro.ubc.ca

ALAN W. IRWIN,[1] ANA M. LARSON, AND STEPHENSON L. S. YANG[1]

Department of Physics and Astronomy, University of Victoria, P.O. Box 3055, Victoria, British Columbia V8W 3P6, Canada

AND

DEREK C. RICHARDSON

Canadian Institute for Theoretical Astrophysics, University of Toronto, 60, St. George Street, Toronto, Ontario M5S 1A7, Canada

Received September 30, 1994; revised February 6, 1995

We have carefully monitored the radial velocities of 21 bright, solar-type stars for 12 years. None has shown any reflex motion due to a substellar companion to an upper limit of between 1 and 3 Jupiter masses (× sin *i*) for orbital periods less than 15 years. We can also rule out companions of more than 3 to 10 Jupiter masses (× sin *i*) at much longer periods based on long-term trends in the radial velocities, limits imposed by astrometry and zones of orbital stability in wide binaries.

When our negative result is combined with other searches, one can say that, so far, no planets of the order of a Jupiter-mass or greater ($\geq 0.001\ M_\odot$) have been detected in short-period, circular orbits around some 45 nearby, solar-type stars. This absence presents an interesting challenge to theories of planet formation.

I. INTRODUCTION

The unequivocal detection of planets revolving about other stars not only would have a philosophical impact but also would be a first step in answering several interesting questions about the transfer of angular momentum during star formation, the stellar and planetary mass function, and the universal proportion of matter bound up in planets. Unfortunately, compared to stars, planets are both faint and of low mass; and as a result they produce only the subtlest of signatures in the apparent motion and image structure of the parent stars. The challenge of detecting such signatures has been summarized in a recent TOPS (toward other planetary systems) report of the NASA Solar System Exploration Division (Burke 1992).

Pulsars are precise clocks, and Wolszczan and Frail 1992 exploited this property to detect two terrestrial planets (each $\sim 3 M_\oplus$) in 98- and 67-day orbits around the 6.2-ms pulsar, PSR B1257 + 12, from a total change in period of only ± 15 psec (1.5×10^{-11} sec). Subsequently, Wolszczan (1994) announced a third companion of lunar mass ($0.015 M_\oplus$). Unfortunately, the Doppler effect in main-sequence stars can be monitored only with a spectrograph and not with a tachometer and stopwatch. Although the stability of spectrographs can be carefully controlled and molecular transitions can be used to provide highly stable wavelength fiducials, the current precision limits us to searching for Jupiter-mass companions.

From 1980 to 1992, we (Campbell *et al.* 1988, Paper I) monitored the radial velocities of 17 bright solar-type dwarf and 4 subgiant stars at the Canada–France–Hawaii 3.6-m telescope (CFHT). Our experimental technique, in which lines of the 870-nm 3–0 vibration–rotation band of hydrogen fluoride are imposed in absorption on the stellar spectra to act as wavelength fiducials, is fully described in Paper I and references therein. The technique is capable of measuring long-term *changes* in the velocity of a star with a precision of ~ 15 m sec^{-1} from a single spectrum. For comparison, the orbit of the Sun about the barycenter, which is dominated by the motion of Jupiter, has a period of 11.9 years with an amplitude of some 13 m sec^{-1}. Thus, by making several observations per year, we could have detected the reflex motion caused by a Jupiter-mass planet orbiting a nearby star provided that the orbital plane was close to the line of sight.

[1] Visiting Astronomer, Canada–France–Hawaii Telescope, operated by the National Research Council of Canada, the Centre National de la Recherche Scientifique of France, and the University of Hawaii.

0019-1035/95 $12.00

Radial velocity searches nicely complement those made astrometrically. The amplitude of the stellar reflex velocity decreases as r^{-1}, where r is the separation of the star from its planetary companion. It is independent of the distance from the observer and varies as sin i, where i is the inclination of the orbital plane to the line of sight. On the other hand, the astrometric amplitude increases linearly with r and inversely as the distance from the observer but it is independent of orbital inclination. Modern astrometric studies claim that as astrometric precision of ~1 marcsec (0.001 arcsec) is possible (Gatewood 1987). With 1 marcsec and 15 m sec^{-1} precision, the cross-over in sensitivity between astrometry and radial velocities for planetary detection occurs at a period of 20 years for a star at 10 pc. Unfortunately, the available time base of astrometric observations of such precision is still too short to be useful in this study.

To date, our planetary search has been the only long-term program on the CFHT. Between three and six pairs of nights per year were allocated over 12 years, apart from a single gap of 6 months in 1983. The ~15 m sec^{-1} precision per observation was achieved to a limiting I magnitude of ~4 for exposures of less than half an hour. The program was completed in 1992. In this paper we present our analysis of 1082 individual differential velocities.

In addition to the dwarf and subgiant stars, we monitored several so-called standard velocity stars all of which were giants or supergiants. Surprisingly, all of these standards proved to be variable in velocity and, in fact, in some cases they showed the signature of velocity variation expected from perturbations by Jupiter-mass companions (Walker *et al.* 1989)! However, in most, if not all cases some intrinsic stellar mechanism is probably the cause of the radial-velocity variations. For γ Cep (Walker *et al.* 1992), a rotational modulation model can explain the radial-velocity period since the chromospheric activity also has the same period. The case of β Gem (Larson *et al.* 1993b) is more difficult because there is only a barely detectable coincident period in the chromospheric activity, and the v sin i value (Gray 1982) seems to rule out the rotational hypothesis. The variability of the giant standards has opened up a highly interesting area of variable star research (see also Hatzes and Cochran 1993).

It is also interesting to note that none of the dwarf stars in our program shows unequivocal evidence of a brown dwarf companion, a result confirmed by the more extensive data of Marcy and Benitz (1989) and Murdoch *et al.* (1993) (see also Latham *et al.* 1989, Cochran *et al.* 1991, and Basri and Marcy 1994).

II. THE OBSERVATIONS

We began our precise radial velocity observations with the coudé spectrograph of the Canada–France–Hawaii 3.6-m telescope in late 1980 and completed them in late 1992. The observing procedure and reduction are fully described in Paper I. Although extensive revisions and corrections have been made to the software (e.g. Walker *et al.* 1990), the basic technique is unchanged.

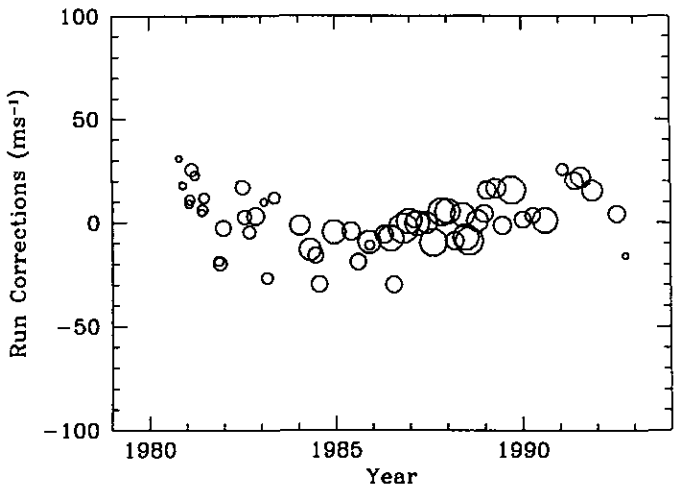

FIG. 1. The systematic offsets in the collective radial velocities between observing runs were applied as corrections to the data and are shown plotted against date of the run. The area of each point is inversely proportional to the square of the internal error estimated for each correction. The mean of these internal errors is 5.6 m sec^{-1}.

We compensate for systematic offsets in the collective differential velocities between observing runs by applying run corrections as described in Larson *et al.* 1993b. The run corrections, which are usually less than 15 m sec^{-1}, are shown in Fig. 1 plotted against date. The area of each point is inversely proportional to the square of the internal error of the point. While the run corrections are probably connected with subtle changes in the instrumental line spread function, we can offer no explanation for their systematic trend. The effect of including or excluding the run corrections is discussed further in Section IV.

The program stars were selected from the brightest dwarf and subgiant stars of solar-types F, G, and K accessible from the latitude of Mauna Kea (+19°). Aside from χ^1 Ori, a newly discovered spectroscopic binary (see Irwin *et al.* 1992a), and α CMi A, known spectroscopic binaries were excluded. The stars are listed in Table I with their Bright Star numbers, Henry Draper number, names, spectral types, and V magnitudes, all taken from the Bright Star Catalogue (Hoffleit and Warren 1991). The fourth column gives the parallax (π_p) in arcseconds (Van Altena *et al.* 1991), the seventh column gives our adopted primary mass (see Paper I, Eq. (1)), and the penultimate column gives the total number of velocities we measured for each star. The final column notes references where stars have already been the subject of papers. The 1082 individual differential velocities and their associated Julian dates are archived with the NSSDC/ADC (the [United States]

TABLE I
The Program Stars

HR	HD	Name	π_p	Sp. type	V	$M/M_\odot$	Obs.	Notes
509	10700	τ Cet	0.283	G8 V	3.50	0.87	68	
937	19373	ι Per	0.094	G0 V	4.05	1.15	46	
996	20630	κ^1 Cet	0.108	G5 Vvar	4.83	0.98	34	
1084	22049	ε Eri	0.306	K2 V	3.73	0.82	65	
1325	26965	o^2 Eri	0.206	K1-V	4.43	0.84	42	
2047	39587	χ^1 Ori	0.111	G0 V	4.41	1.03	38	1
2943	61421	α CMi A	0.286	F5 IV-V	0.38	1.38	98	2
3775	82328	θ UMa	0.069	F6 IV	3.17	1.45	43	
4112	90839	36 UMa	0.078	F8 V	4.84	1.08	56	
4540	102870	β Vir	0.095	F9 V	3.61	1.22	74	
4983	114710	β Com	0.100	F9.5 V	4.26	1.09	57	
5019	115617	61 Vir	0.112	G6 V	4.74	0.98	53	
5544	131156	ξ Boo A	0.149	G8 Ve	4.55	0.92	58	
6401	155885	36 Oph B	0.189	K1 V	5.11	0.78	35	3
6402	155886	36 Oph A	0.189	K0 V	5.07	0.78	26	3
7462	185144	σ Dra	0.177	K0 V	4.68	0.85	56	
7602	188512	β Aql	0.076	G8 IV	3.71	1.30	59	
7957	198149	η Cep	0.074	K0 IV	3.43	1.36	58	
8085	201091	61 Cyg A	0.287	K5 V	5.21	0.67	50	4
8086	201092	61 Cyg B	0.287	K7 V	6.03	0.59	34	
8832	219134		0.150	K3 V	5.56	0.79	32	

Note. 1, Irwin *et al.* 1992a; 2, Irwin *et al.* 1992b; 3, Irwin *et al.* 1995; 4, Larson *et al.* 1993a.

National Space Science Data Center/Astronomical Data Center). (Electronic access to the NSSDC/ADC catalogs can be obtained from URL = http://hypatia.gsfc.nasa.gov/adc.html).

III. VARIATIONS IN VELOCITY

The differential velocities are plotted separately against time in Fig. 2 for each of the stars. The specimen $\pm 1\sigma$ error bar in each plot is a mean for that star and the area of the individual points is proportional to the weight and therefore inversely proportional to the square of the internal error for each point. Prior to plotting the data in Fig. 2, we removed the spectroscopic binary variations of χ^1 Ori and α CMi A, the secular acceleration due to proper motion, and applied the observing run corrections (Fig. 1).

The signal processing electronics of the original RL1872F/30 Reticon diode array were replaced with a lower noise system in 1983.5 (Walker *et al.* 1985) and some residual coma was eliminated from the spectrograph. These changes improved both the precision and observing efficiency and the three stars, θ UMa, 61 Cyg B, and HR 8832 were added to the program at that time.

A notable feature of Figure 2 is that, for most stars, the dispersion in velocities (~20 m sec^{-1}) is very small with no discernible trend except for known visual binaries such as ξ Boo A, 36 Oph A and B, and 61 Cyg A and B. For these stars the predicted velocity variations, as derived from the orbital elements (Worley and Heintz 1983, Irwin *et al.* 1995), the parallaxes and mass ratios of Table I, and the Hershey (1977) mass ratio for ξ Boo, are indicated by solid lines (see also Walker 1993). We interpret deviations of the ξ Boo A and 36 Oph B velocities from the orbital predictions as secular trends (see Section IVb). Since we have successfully detected the large radial velocity changes for the spectroscopic binaries χ^1 Ori and α CMi A (Irwin *et al.* 1992a, b), we conclude that the lack of variability for most stars is not an artifact of the data reduction.

IV. SEARCHING FOR PLANETARY SIGNATURES

While one could look for evidence of eccentric orbits in our data, the likelihood of a false detection would be high because of the limited precision and historical coverage of the observations. On the other hand, with the Solar System planets and satellites, and the pulsar PSR B1257+12 planets all being in nearly circular orbits, it is not unreasonable to limit our search to single giant planets in circular orbits.

The probability of an orbit being inclined to the line of sight at an angle i, P(i), varies as sin i while the detectable

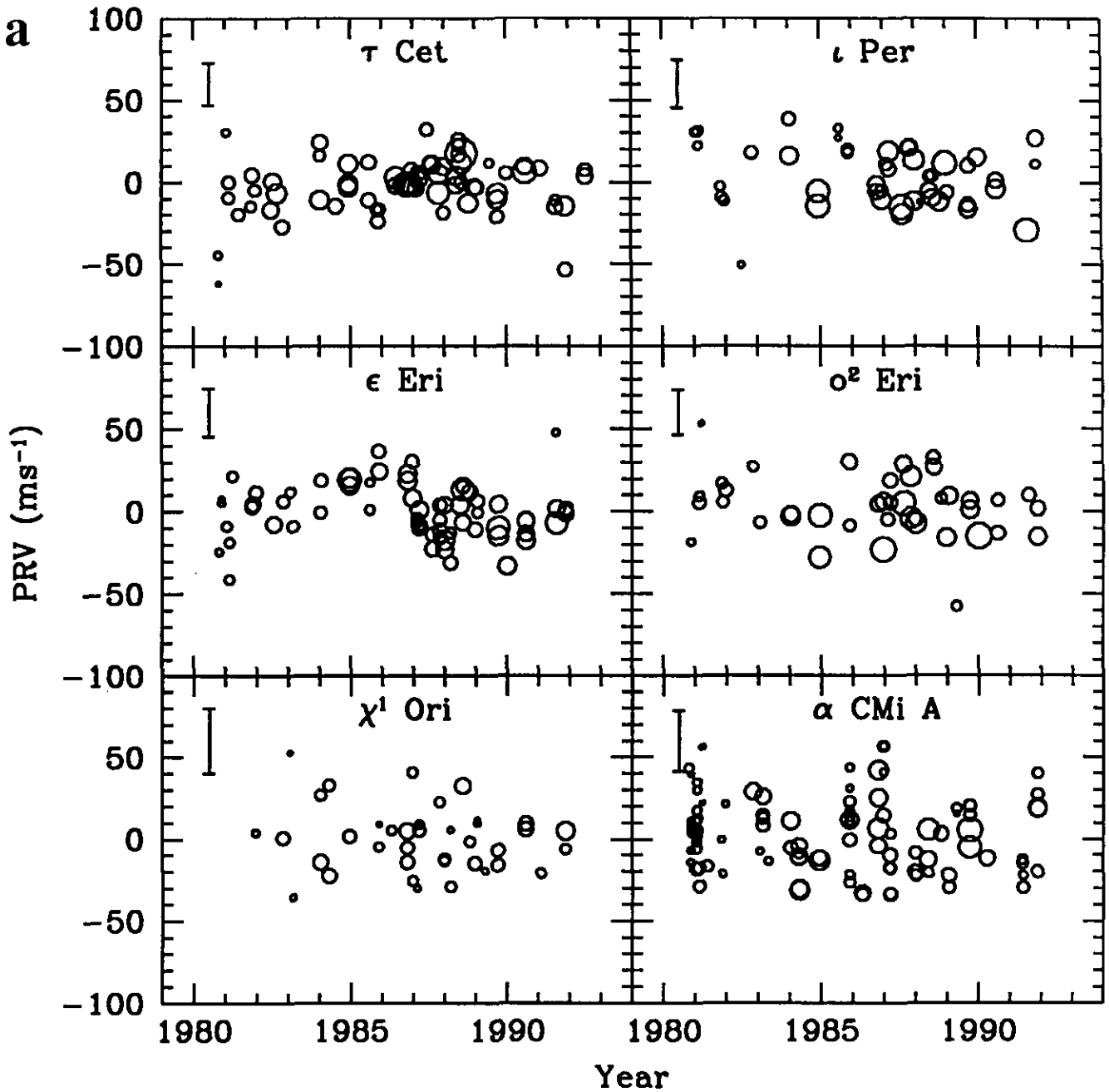

FIG. 2. Differential velocities for the twelve years of the program for each of the 21 program stars after applying run corrections. A $\pm 1\sigma$ error bar indicates the mean internal error for each star while the area of each data point is inversely proportional to the square of the internal error estimated for that point. For κ^1 Cet the index of chromospheric activity, $\Delta EW_{866.2}$ (Larson *et al.* 1993a), is also plotted; in this case the average error (0.067 pm) is less than the smallest point. The solid lines in the plots for the visual binary components ξ Boo A, 36 Oph A and B, and 61 Cyg A and B show the velocity changes predicted from their orbits. For the spectroscopic binaries, χ^1 Ori and α CMi A, the orbital velocity variations have been removed.

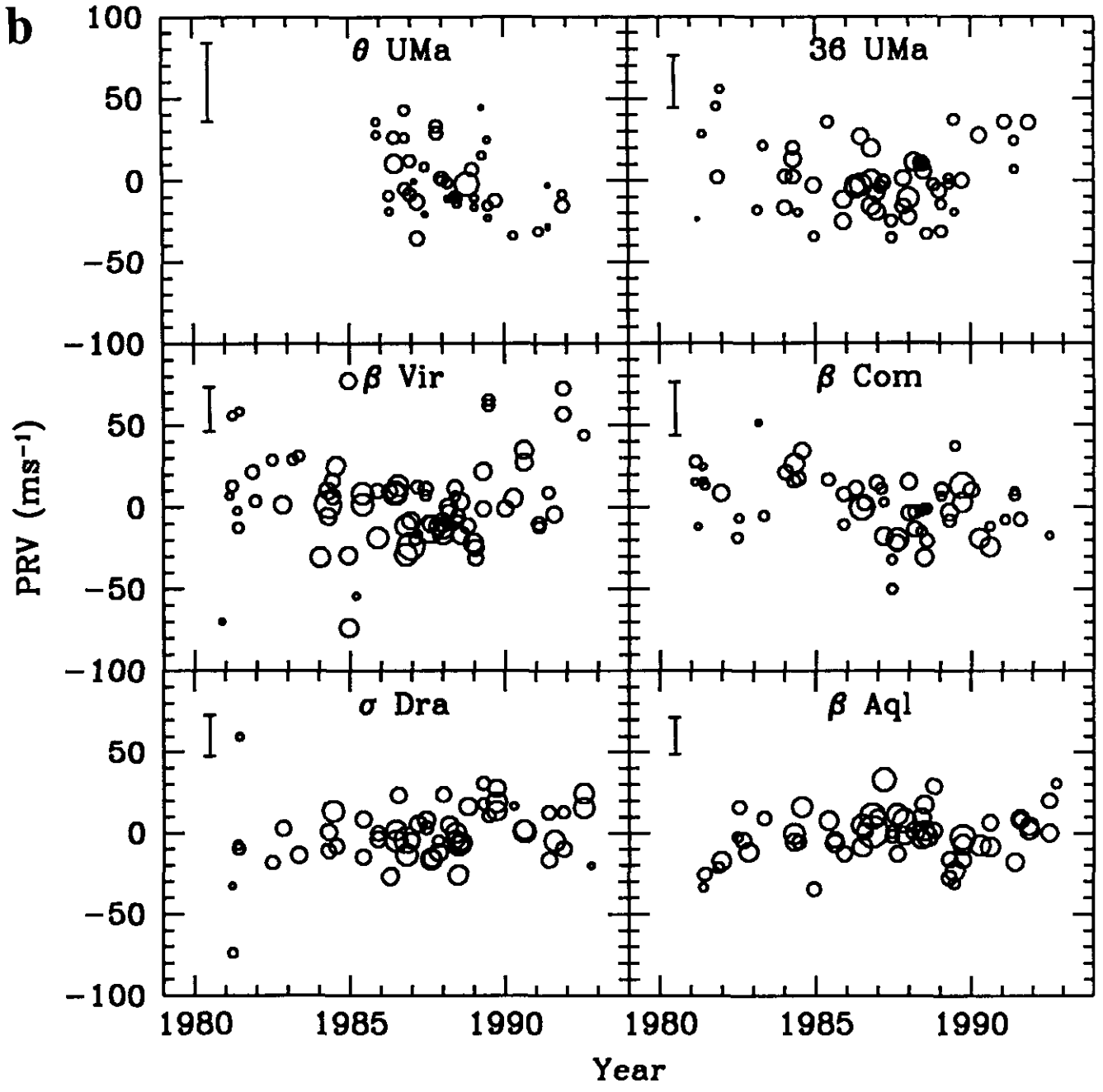

FIG. 2—*Continued*

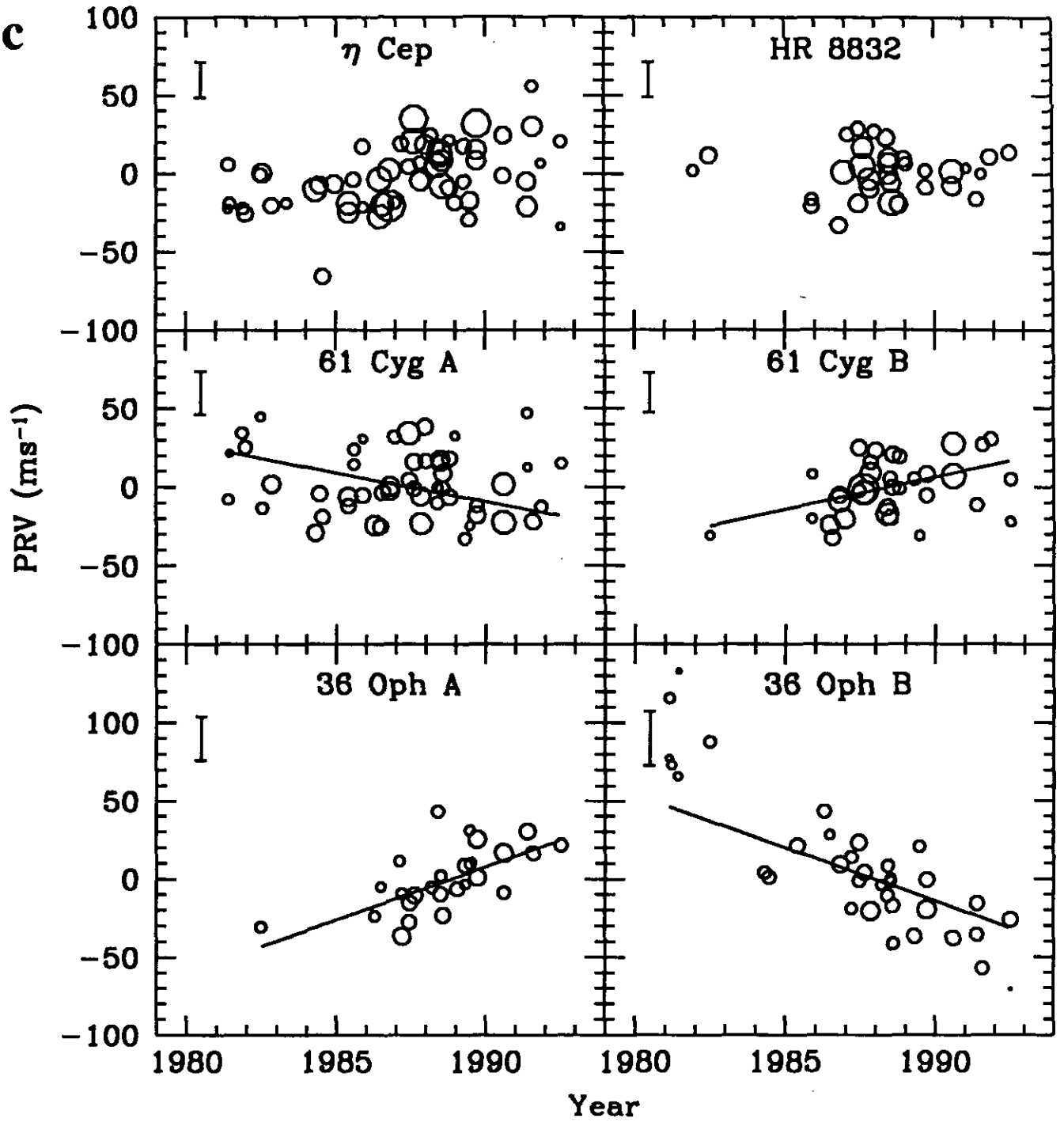

FIG. 2—*Continued*

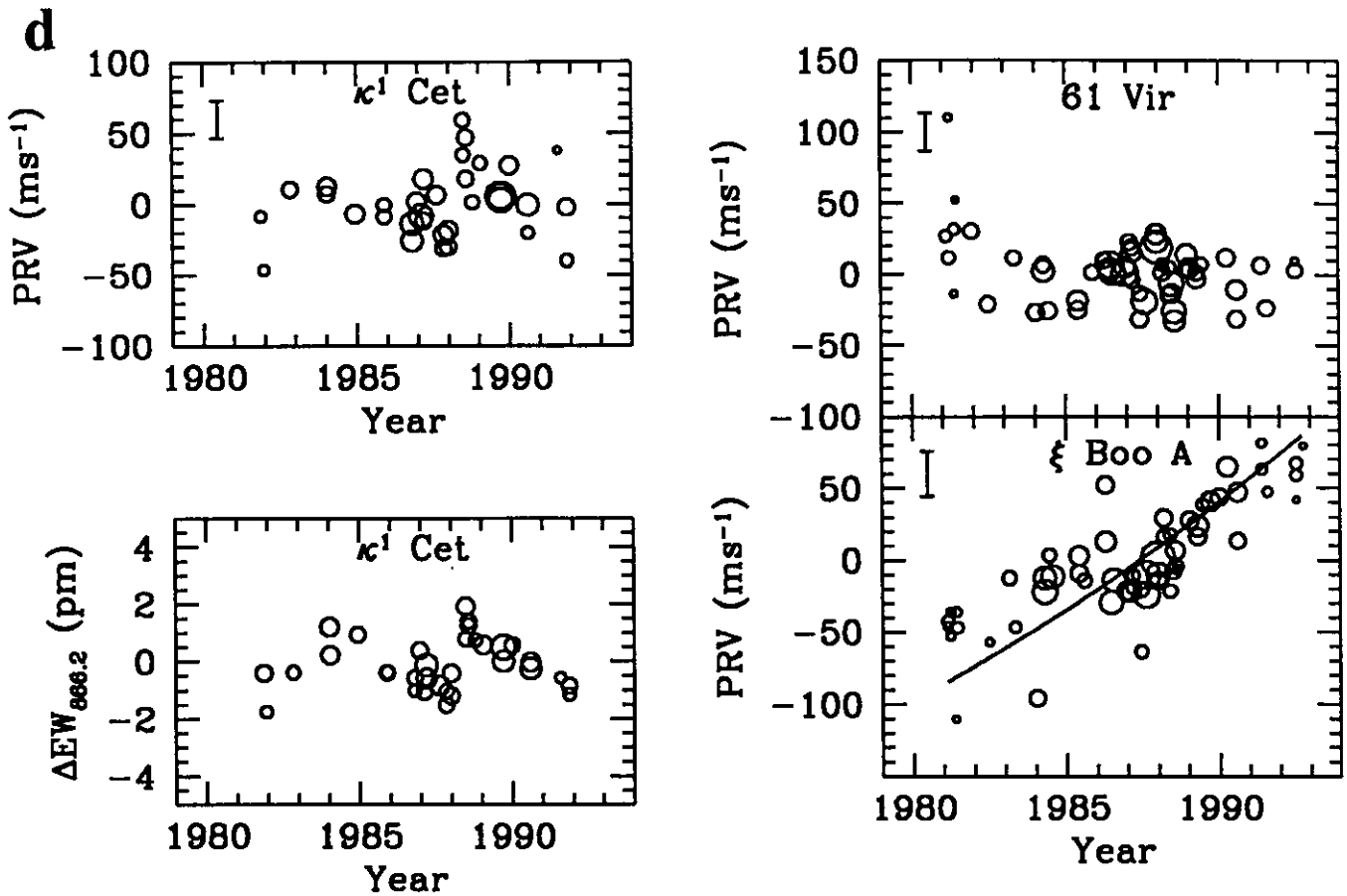

FIG. 2—*Continued*

upper limit to planetary mass goes as $(\sin i)^{-1}$. Thus, although we do not expect to find many planets having orbital planes highly inclined to the line of sight, this study cannot rule out the possibility that such planets exist. More serious would be the existence of any system of two or more giant planets having both similar masses and orbital periods. Such a situation would require a much more extensive data set of higher precision to untangle.

a. Short-Term Periods

Initially, we searched for significant velocity amplitudes in each set of data in Fig. 2 for periods above 100 days using a numerical simulation based on the F statistic (Walker 1993). However, for the current paper, we searched periods above 40 days using a periodogram technique (see the Appendix). Aside from the predicted changes in velocity due to binary motion and the secular acceleration due to proper motion, no longer-term trends were removed from the data before generating the periodograms.

The technique is illustrated for ε Eri, η Cep, and for the giant K0 star, γ Cep (see Walker *et al.* 1992) in Fig. 3 where the periodogram is shown as a function of frequency ($\equiv$ period^{-1}) both for the run corrected (solid line) and uncorrected data (dashed line). For γ Cep a trend corresponding to a 50-year binary orbital motion has been removed from the data. The horizontal lines are the estimates (see Appendix) of the 99% confidence limit expected from random data.

The run-corrected radial velocities are replotted as a function of phase in Figure 4 for the 9.88-year period for ε Eri, the 0.45-year period for η Cep, and the 2.52-year period for γ Cep. The data are also shown binned at intervals of 1/10th of the period.

The periods exhibited in Fig. 4 for ε Eri and η Cep are among the most significant for the stars in Table I. There is also a significant peak at 56 days for ε Eri (see Fig. 3). We have established that this peak and the 9.88-year peak are aliases of each other, and we cannot distinguish which is the true period. The 0.45-year period of η Cep requires further investigation. We note that this star is substantially

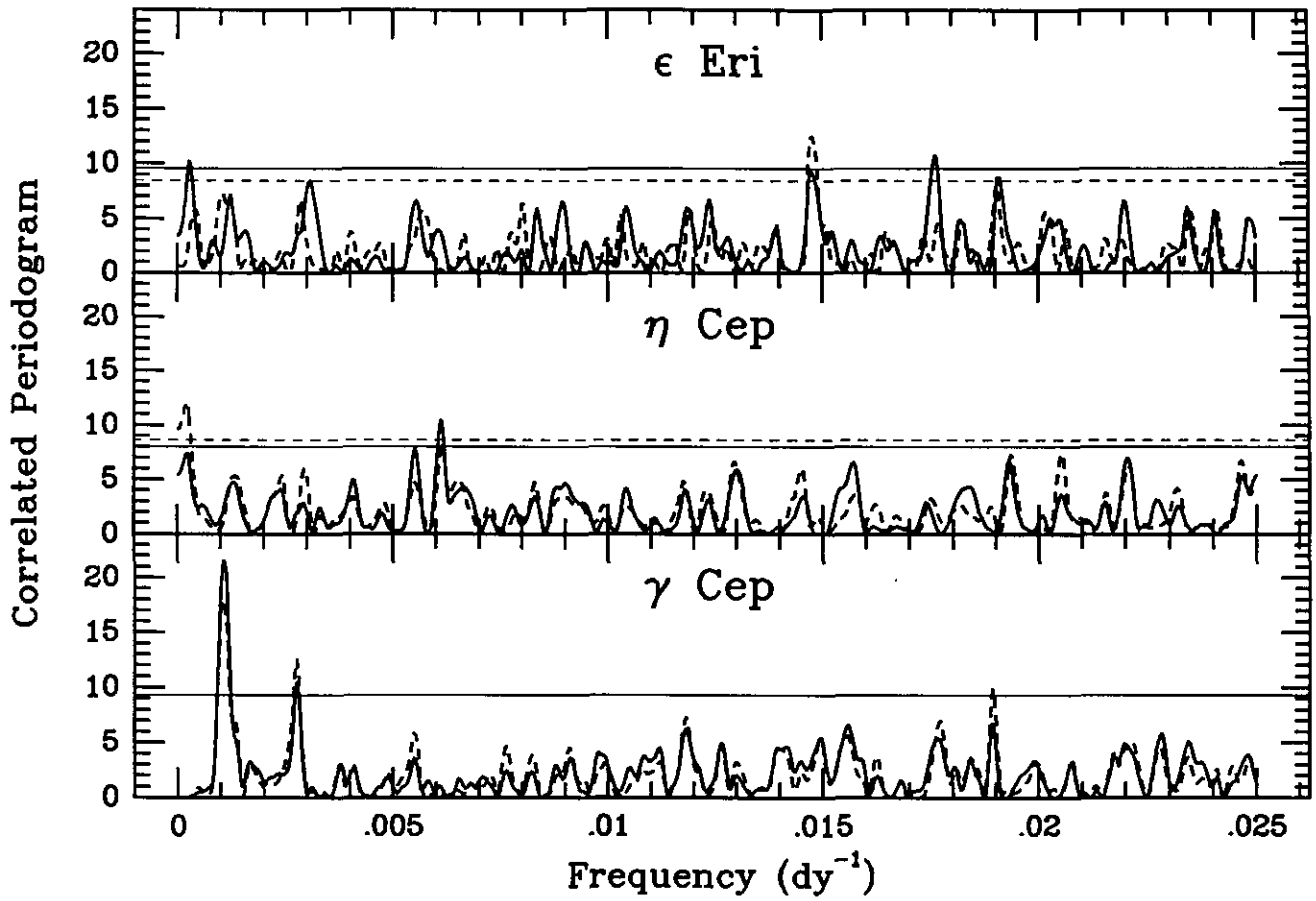

FIG. 3. The correlated periodogram as a function of frequency (≡ period^{-1} for ε Eri, η Cep and γ Cep. The horizontal line is an estimate of the 99% confidence limit expected from random data (see Appendix). The dashed lines correspond to the data without run corrections, the solid lines to the run corrected data. For γ Cep, the uncorrected and corrected confidence limits are the same, and a 50-year binary variation has been removed.

evolved (more than 3 mag above the main sequence) so this periodicity, although marginal, may be related to the periodicities of the giants where at least some of the results can be explained as a rotational phenomenon. α CMi and 61 Vir exhibit statistically significant periods at 1 year which are probably artifacts of the annual observing cycle, and we are investigating this effect further.

In contrast to the results for γ Cep, the values of the periodogram peaks for ε Eri and η Cep in Fig. 3 depend on our run corrections. We feel that these results are too marginal to qualify as a convincing periodicity. These periodogram analyses are the basis for our conclusion that we have detected no unequivocal planetary companion signatures in our data but, rather, can set interesting mass limits to any such companions. The latter point is taken up in Section V.

It is worth commenting here on the velocity curve for κ^1 Cet. The velocities executed a marked S-shaped excursion between 1988 and 1990 which could have arisen from dynamical perturbation by a planet in a highly eccentric orbit. However, the coincident S-shaped variation in the chromospheric index $\Delta EW_{866.2}$ (as defined in Larson *et al.* 1993a and plotted for κ^1 Cet in our Figure 2) makes it much more likely that the changes between 1988 and 1990 were connected to chromospheric activity on the star.

b. Secular Trends

Many of our program stars show long-term trends in velocity which could be formally interpreted as perturbations by planets in orbits with periods of more than 20 years. Before testing for secular trends in the velocities of these stars, we removed the accelerations predicted from both binary and proper motions. We excluded χ^1 Ori and α CMi A from the analysis because small secular trends could be absorbed into the fit for the spectroscopic binary elements which are heavily influenced by our velocities.

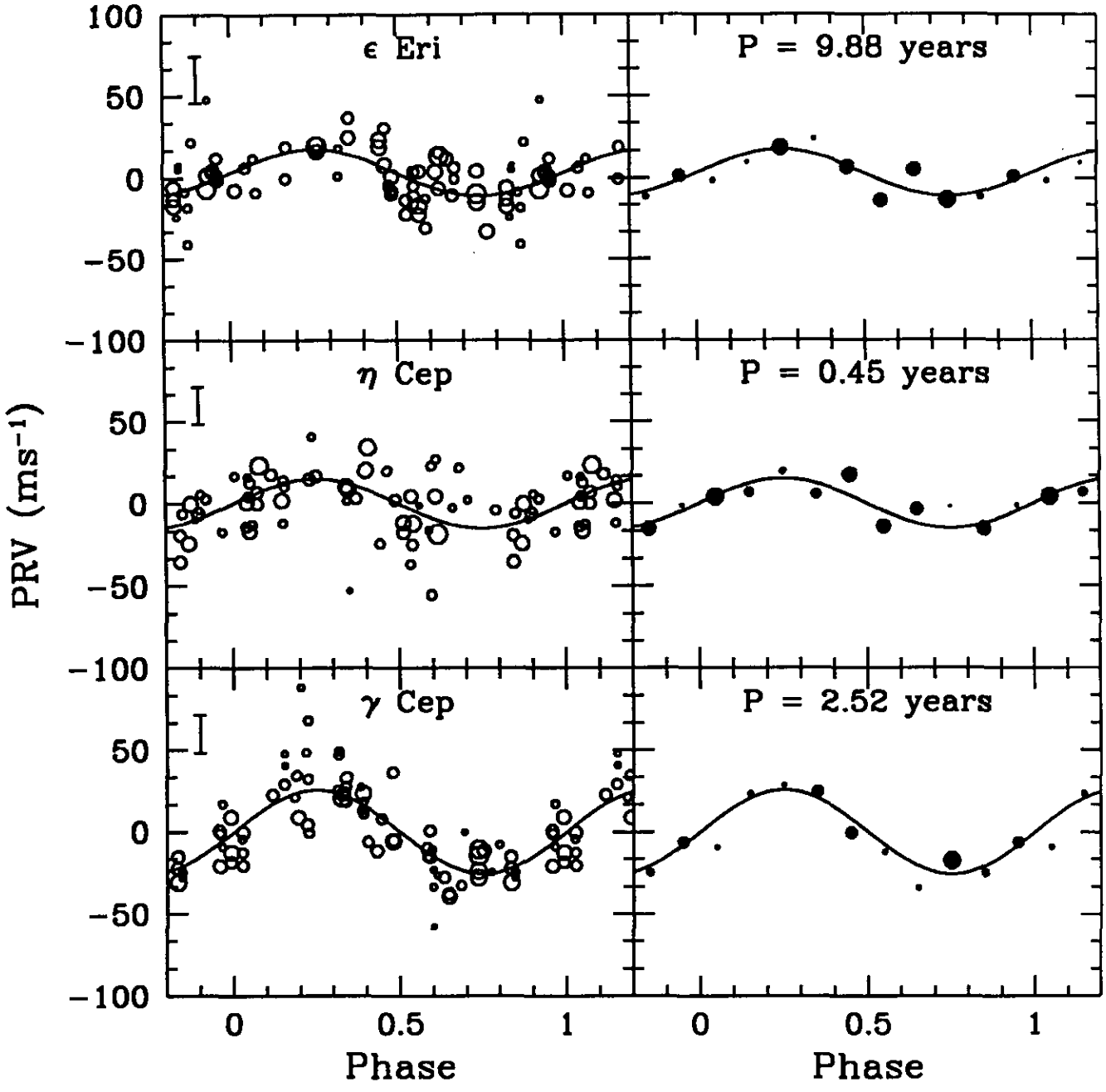

FIG. 4. The run-corrected radial velocity data of ε Eri, η Cep, and γ Cep replotted as a function of phase for the indicated periods. For γ Cep a 50-year binary variation has been removed. The data are also shown binned at intervals of 1/10th of the period.

TABLE II
F Test Results for Secular Trends in the Radial Velocity

Name	Sp. type	ν	Uncorrected $F_{2,\nu}$	Uncorrected False alarm	Corrected $F_{2,\nu}$	Corrected False alarm
τ Cet	G8 V	65	4.5103	0.0146	3.8017	0.0275
ι Per	G0 V	43	1.7058	0.1937	1.0829	0.3477
κ^1 Cet	G5 Vvar	31	3.1095	0.0588	0.3543	0.7045
ε Eri	K2 V	62	0.6590	0.5210	3.7302	0.0295
o^2 Eri	K1-V	39	1.2127	0.3084	0.2430	0.7854
θ UMa	F6 IV	40	0.1254	0.8825	3.7147	0.0331
36 UMa	F8 V	53	22.3067	0.0000	9.0571	0.0004
β Vir	F9 V	71	20.7980	0.0000	6.7746	0.0020
β Com	F9.5 V	54	6.2784	0.0035	5.5248	0.0066
61 Vir	G6 V	50	3.2069	0.0489	1.1808	0.3154
ξ Boo A	G8 Ve	55	8.6377	0.0005	10.0727	0.0002
36 Oph B	K1 V	32	9.0155	0.0008	7.6699	0.0019
36 Oph A	K0 V	23	2.4071	0.1124	0.4388	0.6501
σ Dra	K0 V	53	11.2479	0.0001	3.2433	0.0469
β Aql	G8 IV	56	8.5572	0.0006	1.4976	0.2325
η Cep	K0 IV	55	13.8910	0.0000	6.4257	0.0031
61 Cyg A	K5 V	47	7.8998	0.0011	3.0284	0.0579
61 Cyg B	K7 V	31	1.9020	0.1663	0.4499	0.6418
HR 8832	K3 V	29	2.6494	0.0877	0.2280	0.7976

One can check for secular trends by using the *F* test to compare the weighted sum of squares of the residuals for a mean model and a model with a parabolic trend. Table II gives the *F* test results (false alarm probabilities calculated using Eq. (6.3.11) of Press *et al.* 1986) for both the run-corrected and the uncorrected data. In most cases the run-corrected results show less significant variations (larger false alarm probabilities). We feel that this vindicates the use of the run corrections in Fig. 1; if our run corrections had contained an invalid long-term trend, we would have expected the corrected data to have consistently more significant variations, not less.

We should be able to relate the *F* test results to the correlated periodogram results since the two statistics are so closely related (see Eq. (A3)). The correlated periodogram evaluated at a period of 100 years ranged from 5.2 for η Cep (see Fig. 3) to 7.4 for ξ Boo A. None of the corresponding periodogram false alarm probabilities is less than 0.01 (i.e., the low-frequency periodogram values do not exceed the 99% significance level). The latter result seems to be in direct contradiction with the *F* test results but is in fact a consequence of the large frequency range (corresponding to periods between 40 days and 100 years) that was searched when calculating the periodogram false alarm probability. If a consistent pattern (such as a low-frequency rise) shows up in periodograms of independent data it is legitimate to narrow the frequency search about the pattern (Larson *et al.* 1993b). For narrowed frequency searches there are fewer chances for the randomized data to produce large peaks in the periodogram and the false alarm probabilities drop. The conclusion is that the *F* test results are a reliable indicator of long-term activity so long as the implied narrow frequency search is legitimized by long-term activity being exhibited for more than one or two of the stars observed. In the present case, there seems to be a consistent pattern of apparent long-term activity for approximately one-third of our stars (approximately one-half of our stars if we do not apply run corrections) which cannot be dismissed on statistical grounds.

Table II contains members of the binary systems ξ Boo, 36 Oph, and 61 Cyg, and it is worth investigating whether errors in the 3-dimensional orbit parameters would generate an apparent long-term systematic trend in radial velocity. Our investigations are not yet complete for ξ Boo and 61 Cyg. We find (Irwin *et al.* 1995) that unrealistically large variations in the adopted parallax, sum of masses, mass ratio, or visual-binary elements would be required to significantly alter the predicted orbit slopes illustrated in Fig. 2 for 36 Oph A and B.

The binaries also allow us the unique opportunity of determining the maximum period for a planetary companion that may be orbiting one of the binary components. A key parameter in orbital stability analysis is $Q = a(1 - e)/a_c$, where e is the binary orbit eccentricity, $a(1 - e)$ is the binary distance of closest approach, and a_c is the semimajor axis of the planetary companion of one of the binary members. For binary mass ratios near unity, Q must be greater than about 4 in order for the planetary orbit to be dynamically stable (see Donnison and Mikulskis 1992, Fig. 6). This means that the maximum stable planetary companion periods for members of the 36 Oph, ξ Boo, and 61 Cyg binaries would be about 2, 8, and 60 years, respectively. (Similarly, the maximum planetary companion periods for χ^1 Ori and α CMi A are about 2 and 3 years, respectively.)

We would now like to comment on the six stars (36 UMa, β Vir, β Com, ξ Boo A, 36 Oph B, and η Cep) in Table II with the most significant long-term variations (corrected false alarm probabilities less than 0.01).

The apparent long-term trends for ξ Boo A and especially for 36 Oph B are unlikely to be due to planetary companions because of the dynamical stability limits on the maximum period described above. Clearly, none of the long-term trends for the six stars can correspond to a simple acceleration of the entire stellar surface layers; otherwise, the increase in radius would be so great that there would be large photometric changes which have not been seen. An alternative possibility is that the convective blue shift (caused by the bias of hot rising elements having larger intensity than cool falling elements) changes slowly with time.

Because convective and chromospheric activity are related for dwarf stars, there might be some correlation between our velocity trends and chromospheric activity but we have found none. Only in the case of κ^1 Cet does chromospheric activity seem to coincide with a short-term velocity change (Fig. 2). Given the variety of chromospheric behaviour of the stars and the limited time coverage and precision of our observations, we are not in a position to distinguish a planetary perturbation from other plausible explanations for such long-term trends. Here we simply caution that there could be planetary perturbations below the upper limits set in the next section.

η Cep is an example of an evolved star that shows a secular trend. As we emphasized earlier, the radial velocity variations of this star may be related to those of the two giants β Gem and γ Cep. It is interesting that, despite the lack of a long-term trend in the velocities of β Gem, its chromospheric activity does have a parabolic trend (Larson *et al.* 1993b).

V. UPPER MASS LIMITS TO PLANETARY COMPANIONS

We describe in the Appendix how we establish useful upper limits to the mass ($\times \sin i$) of possible companions to our program stars as a function of period. In addition, we calculate formal astrometric maximum masses (independent of sin i) from Eq. (7) in Paper I,

$$m = 1.05(\alpha_L/\pi_p)(M_*/P)^{2/3}, \quad (1)$$

where m is the companion mass in Jupiter masses, α_L is the assumed upper limit in milliarcseconds to astrometric variations, π_p is the parallax in arcseconds, P is the period in years, and M_* is the stellar mass in solar masses.

The maximum mass ($\times \sin i$) allowed by our radial velocities for periods less than 100 years are plotted on a log–log scale for each star in Fig. 5 for both the run corrected (solid line) and uncorrected (short dashes) data. The arrows for the members of binary systems indicate the maximum companion period derived from dynamical stability arguments (see above). In addition, we show the astrometric mass limits (long dashes) derived from Eq. (1) for $\alpha_L = 10$ marcsec, which is typical for astrometric measurements of sufficient time base. Gatewood (private communication 1993) has reported an astrometric limit of 1.4 marcsec for ε Eri. With astrometric data of this latter precision over the next decade, the longer periods in Fig. 5 will increasingly be constrained by the astrometry.

From Fig. 5 it can be seen that our radial velocities set upper limits of ≤ 1 and ≤ 3 Jupiter masses ($\times \sin i$) for the possible mass of any companion to most of our stars for periods ≤ 1 and ≤ 15 years, respectively. For half of the stars, the limit is already less than a Jupiter mass for periods of less than 2 years. Combined with the $\alpha_L = 10$ marcsec limit our radial velocities impose a limit of ≤ 10 Jupiter masses ($\times \sin i$) for periods up to 100 years except for χ^1 Ori and θ UMa, and in most cases the limit is closer to 3 Jupiter masses ($\times \sin i$). For all of the periods shorter than 15 years the upper mass limit is improved by using the run-corrected data and this is also true for the majority of the longer periods.

VI. THE ABSENCE OF JUPITER-MASS PLANETS

Table III summarizes the successes and limits, to date, of Doppler searches for planets by ourselves and other groups. Although the Lick group has observed some 65 stars, data reduction is complete only for 25 (Marcy, private communication, 1995). Apart from the study of the millisecond pulsar, all of the targets are solar-type main sequence or subgiant stars. In each technique a set of natural or artificial wavelength fiducials such as hydrogen fluoride, iodine vapor, telluric oxygen, or Fabry–Perot etalon fringes is imposed in the stellar spectra.

There are many stars in common between the programs. Nonetheless, one can say that, to an upper limit of a few Jupiter masses ($\times \sin i$), no planets have been discovered as companions to about 45 nearby stars. Even more surprising, none of the programs cited in Table III has detected a brown dwarf (0.02 to 0.08 $M_\odot$) companion.

When we began this program over 14 years ago, we fully expected that, with sufficient precision, we would find several candidate giant planets. Not only is the Solar System dominated dynamically by Jupiter, but simulations such as those of Isaacman and Sagan (1977) suggested that a Solar System-like distribution of planetary masses and Bode's Law orbits would arise naturally around single stars. Very recently, Boss (1995) has predicted that Jupiter-mass planets will tend to form at distances of 4 to 5 AU around low-mass (0.1 to 1 $M_\odot$) stars. The distance is largely dictated by conditions in the protoplanetary disc rather than by the mass of the star which means that the period of revolution would decrease with the mass of the parent star. The absence of giant planet detections in Table III would seem to challenge these conclusions (although only our survey has sufficient time base) and suggests that we shall now have to improve the precision of Doppler searches and look for lower-mass companions similar to Uranus.

Theoreticians say that they will be satisfied with nothing less than a system of planets because there is already ample evidence for protoplanetary discs around many stars. Lagage and Pantin (1994) achieved a resolution of 5 AU in 10-μm images of the disc around β Pic and the dust distribution was asymmetrical and significantly depleted within 40 AU of the central star. They interpret this as

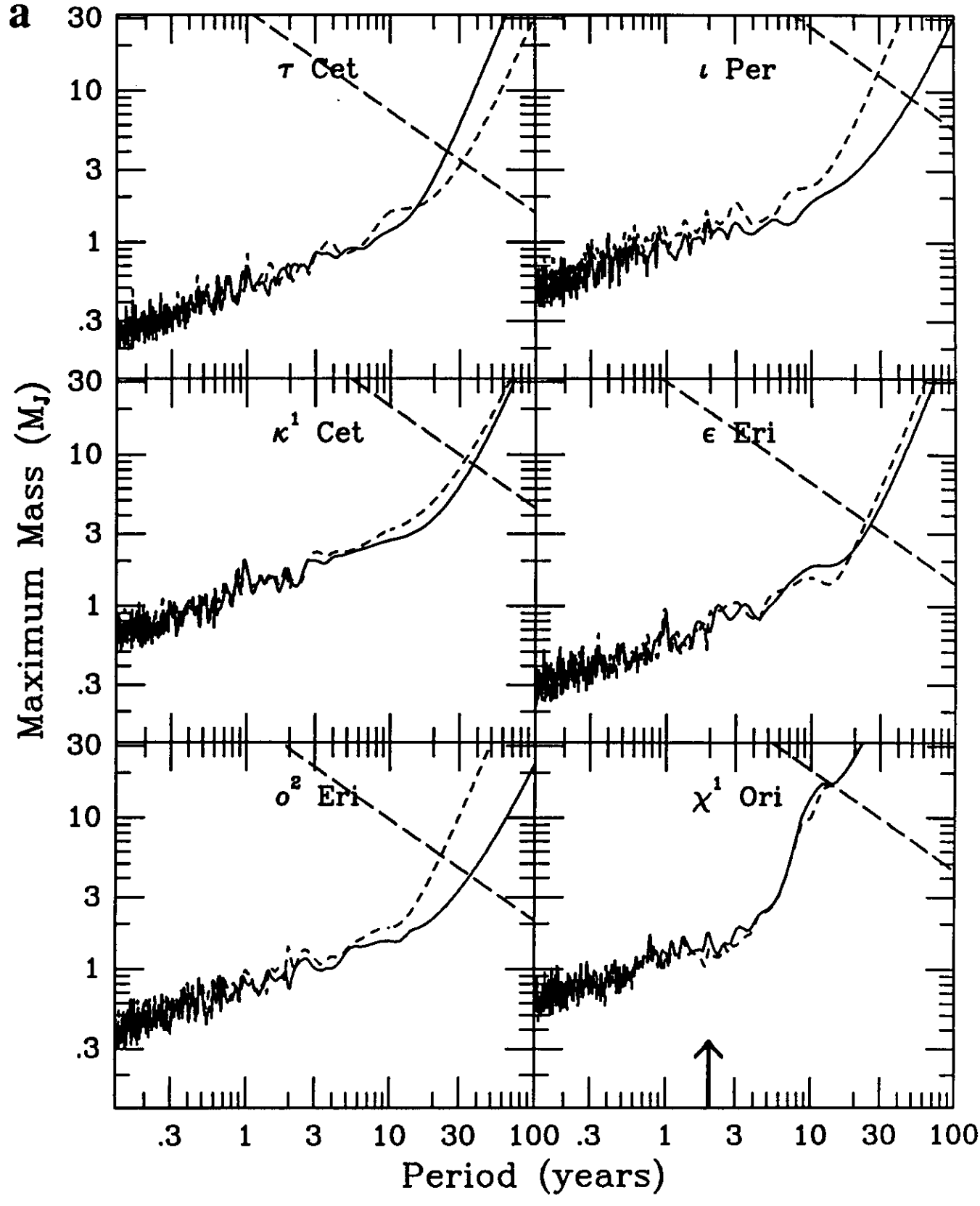

FIG. 5. The maximum allowable companion mass to our program stars for periods between 40 days and 100 years. The solid line shows the maximum mass ($\times \sin i$) from the periodogram technique described in the Appendix using the run-corrected data, and the short-dashed line is for the uncorrected data. The line with the long dashes in the astrometric limit for 10-marcsec precision. For the stars in binary systems, the arrows indicate the maximum companion period allowed by dynamical stability arguments (see text).

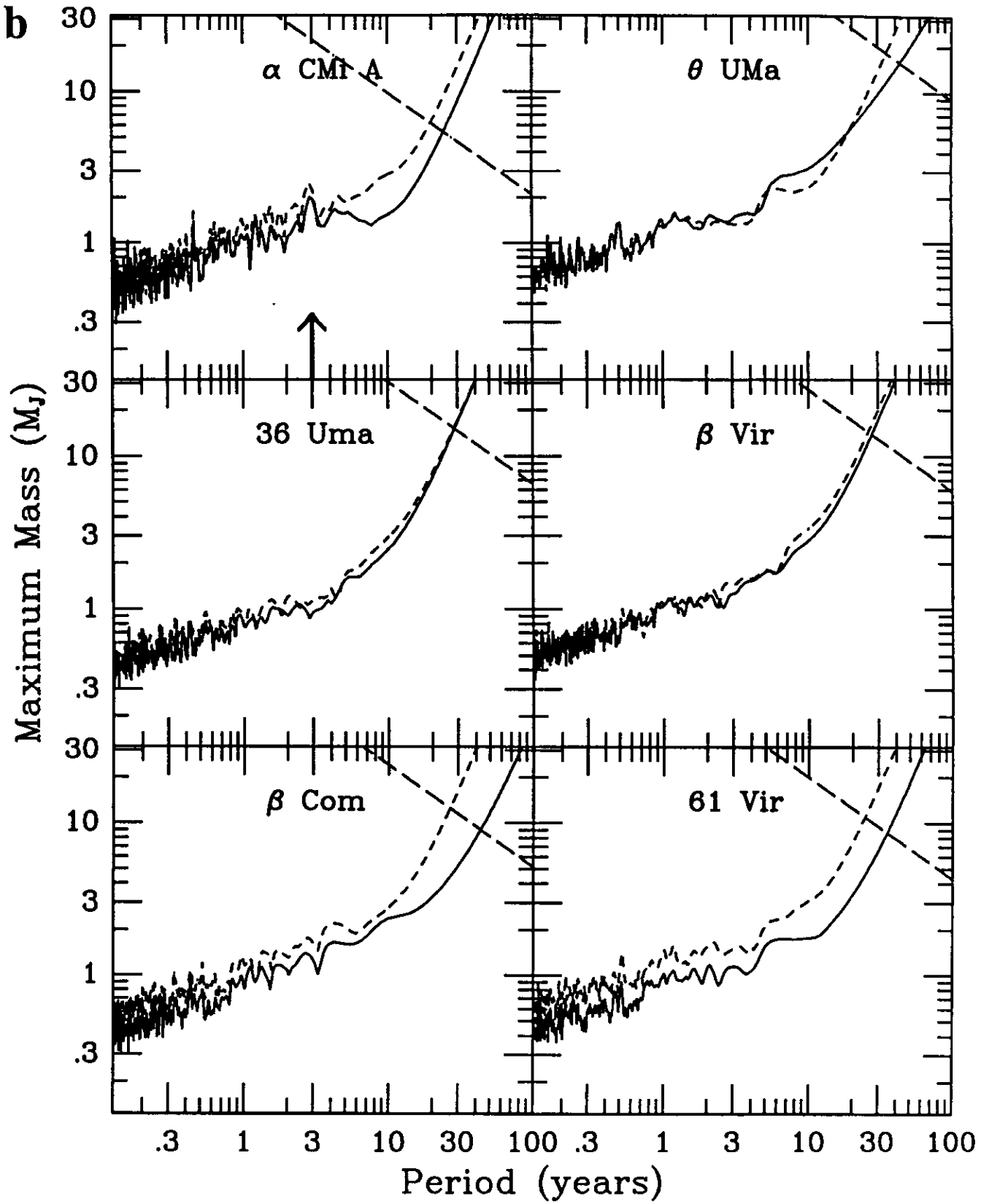

FIG. 5—*Continued*

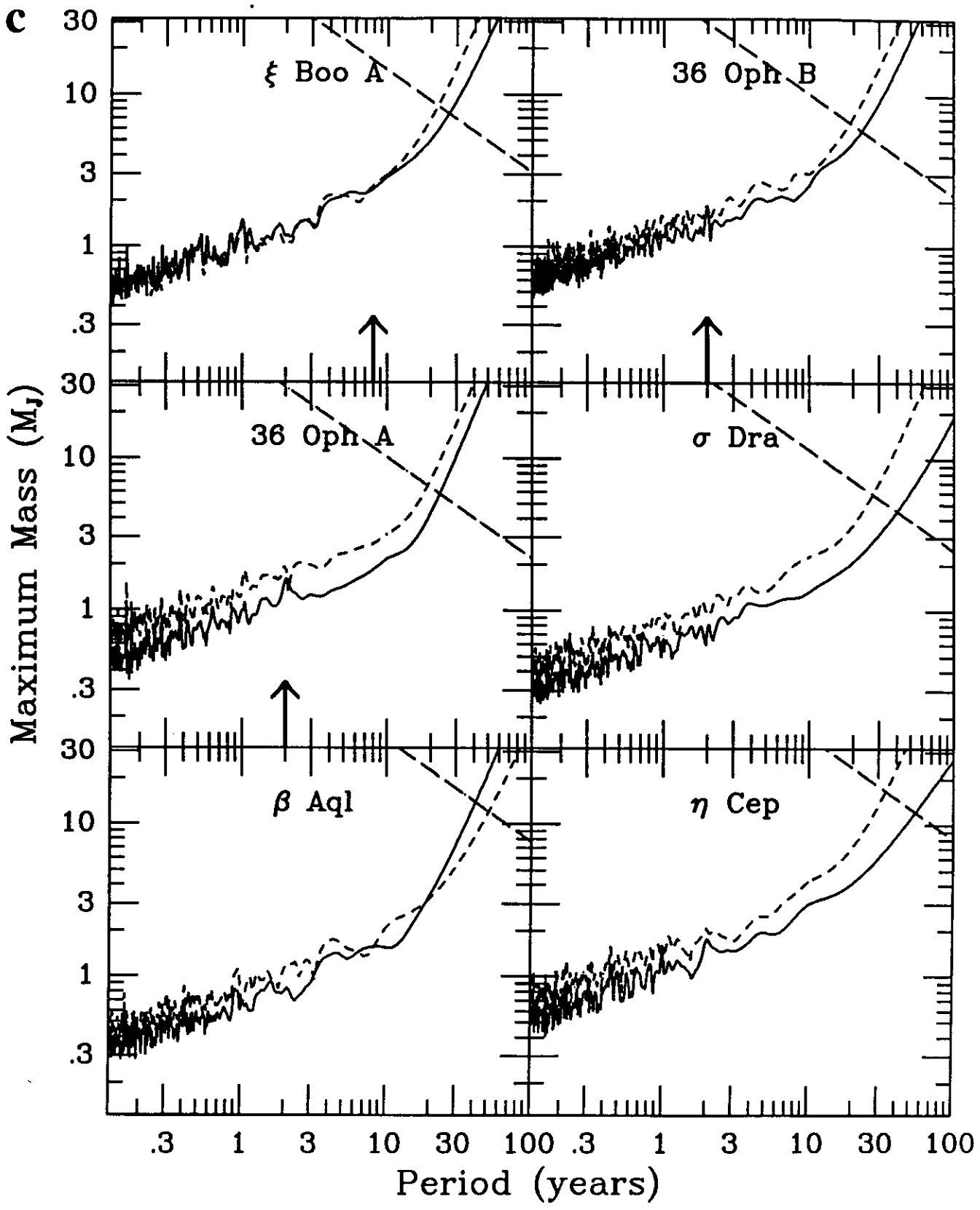

FIG. 5—*Continued*

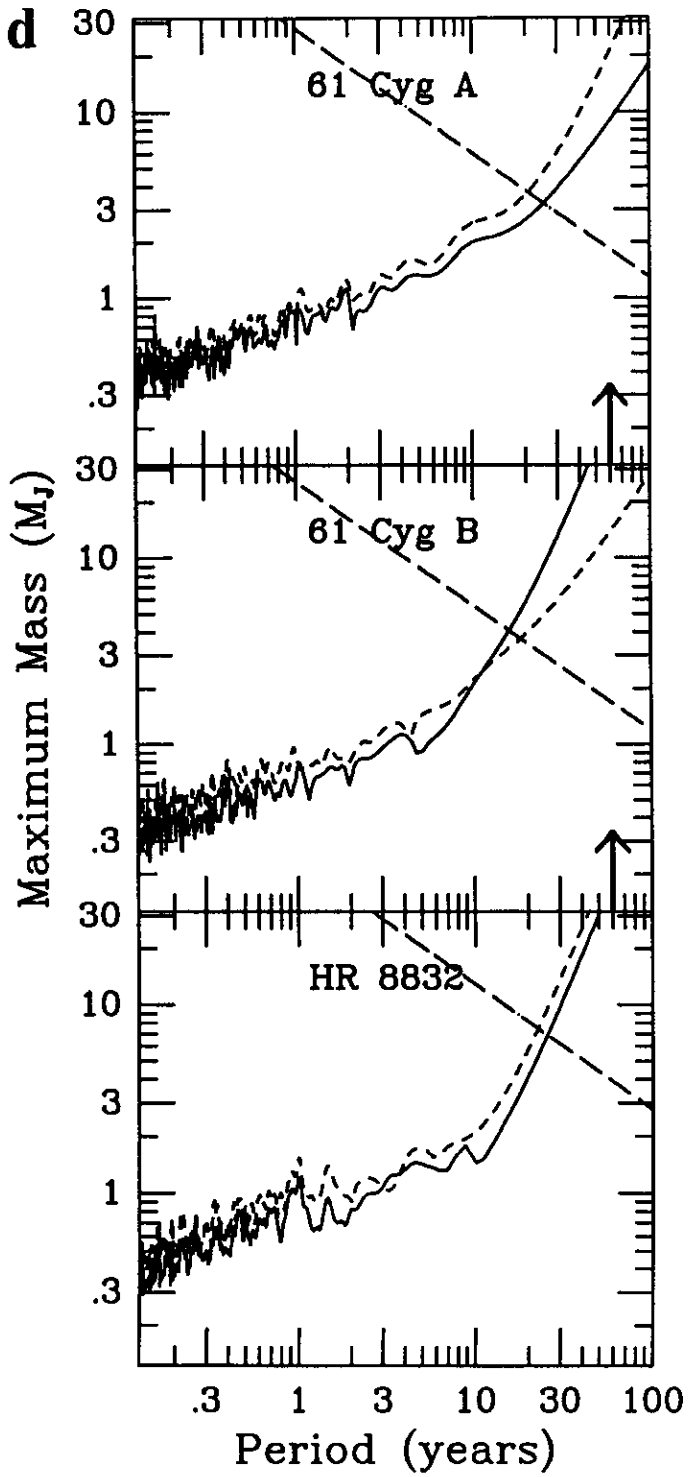

FIG. 5—*Continued*

evidence for an Earth-mass planet in a slightly eccentric orbit at some 40 AU. The millisecond pulsar, PSR B1257+12, at least seems to demonstrate that terrestrial mass planets do exist around neutron stars!

APPENDIX:

The Maximum Companion Mass Allowed by Radial Velocities

We formally define the maximum allowed companion mass as the upper-tailed 99% confidence limit on the possible companion mass allowed by radial velocity data. For circular orbits the companion mass m (Jupiter masses) is related to the sinusoidal amplitude K (m/sec) of the radial velocity by (see Paper I),

$$m \sin i = (1/28.4) K P^{1/3} M_*^{2/3}, \tag{A1}$$

where P is the period (years), M_* is the primary mass (solar masses), and i is the angle of inclination. We use numerical simulations to derive the amplitude confidence limit and transform this limit to the maximum allowed companion mass using Eq. (A1).

We start with a least-squares fit to the observed data. The fit provides the residual/sigma distribution and the parameters of the parent model (in the simplest case, a mean) that are used in the numerical simulation. We add pseudorandom errors to the parent model to derive 100 simulated data sets which are subsequently fitted to obtain the distribution of the amplitude and its confidence limit. The pseudorandom errors are derived in such a way (see Irwin *et al.* 1989, Eq. (4)) that the simulated data sets have an error/sigma distribution that is the same as the residual/sigma distribution derived from the original least-squares fit. Furthermore, the simulated data sets have the same parent model, epochs, and relative weights as the observed data.

Our technique for finding the maximum amplitude confidence limit is based on a statistical analysis of the periodograms of simulated data sets. The Lomb–Scargle periodogram and its generalizations (see below) are equivalent to a least-squares fit of a model consisting of the parent function plus a sinusoid with fixed period. For each of our simulated data sets we find the maximum periodogram value for all periods from 40 days to 100 years. (The search over a substantial period range is essential for helping to account for the effects of aliasing.) We find the 99% confidence limit for the maximum periodogram value from the distribution of 100 values determined from the simulated data sets. We define the maximum amplitude confidence limit such that when the sinusoid with the least-squares phase and this amplitude is subtracted from the observed data, the periodogram of the result is equal to the maximum periodogram confidence limit. We use Brent's method (Chapter 9.3 in Press *et al.* 1986) to solve for this maximum amplitude at each period.

We define the correlated periodogram by

$$P_c(f) = (n - m)(\chi^2_{\mathfrak{P}} - \chi^2_{\mathfrak{M}})/(2\chi^2_{\mathfrak{P}}), \tag{A2}$$

where $\chi^2_{\mathfrak{P}}$ is the weighted sum of squares of the residuals for a least-squares fit of the parent function (in the simplest case a mean) with n observations and m parameters and $\chi^2_{\mathfrak{M}}$ is the weighted sum of squares of the residuals for a least-squares fit of the model function (≡ parent function + sinusoid of fixed frequency $f = 1/P$). The correlated periodogram is obviously related to the F statistic that is commonly used to measure the improvement in the fit due to the addition of the two extra sinusoid parameters in the model. In the present case we have

$$P_c(f) = \frac{(n - m)F_{2,n-m-2}}{n - m - 2 + 2F_{2,n-m-2}}. \tag{A3}$$

In general, the parameters of the parent function correlate with the amplitude and phase of the sinusoid in the model function fit. Under certain conditions (e.g., a high-frequency sinusoid and a parent function

TABLE III
Doppler Searches for Planets

Group	Technique	σ_{RV}	Stars	Time base (years)	Detections
ms pulsar[a]	Timing	0.1 mm sec^{-1}	1	3	0.015, 2.8, 3.4 $M_\oplus$
UBC/UVic[b]	HF	15 m sec^{-1}	21	12	None > 1–2 M_J
Texas[c]	O_2, I_2	15 m sec^{-1}	27	6	None
Lick[d,e]	I_2	15 m sec^{-1}	26	3	None > 3 M_J
Arizona[f]	F-Perot	30 m sec^{-1}	16	8	None

[a] Wolszczan 1994.
[b] This paper.
[c] Cochran and Hatzes 1993.
[d] Marcy and Butler 1992a,b.
[e] Marcy 1995.
[f] McMillan *et al.* 1994.

that changes slowly with time), the correlation is small and essentially the same periodogram results are obtained by freezing all parameters of the parent function when fitting the model function. In this case, the correlated periodogram reduces to the weighted periodogram which can be calculated with a relatively simple formula (Irwin *et al.* 1989, Eq. (5)). If uniform weights are assumed, the weighted periodogram reduces to the well-known Lomb–Scargle periodogram.

In the present numerical simulations we have extended the period search to well beyond the typical epoch range of 12 years. For periods much larger than the epoch range, the amplitude and phase of the derived sinusoid will clearly correlate with the mean of the parent function. If the mean were artificially frozen in the fits as in the weighted or Lomb–Scargle periodogram case, then the derived periodogram values would be too low for the longer periods. It is for this reason that we invented and used the correlated periodogram for the present numerical simulations.

ACKNOWLEDGMENTS

This work was inspired by the pioneering measurements of small spectral line shifts by John Glaspey and Gregory Fahlman. Both have continued to be interested in the project and, in John's case, took an active part in the observations. Bruce Campbell's energy and initiative established and sustained the program in its initial stages and many others have contributed over the years. At UBC, Dieter Schreiber built the gas handling system, Ron Johnson built the detectors, and John Amor helped with the observations and in an early stage of the data reduction. AT CFHT, Derek Salmon and Tom Gregory together with other members of the optical group carefully collimated the coudé and spectrograph optics before each run. Ken Barton, Norman Purvis, and John Hamilton always gave excellent support as night assistants. David Bohlender helped with the program while at UBC and later when he joined the staff of the CFHT. A.W.I. is grateful to Jim Hesser for providing facilities at the Dominion Astrophysical Observatory to complete part of this work. At the University of Victoria, Cherie Goodenough helped with the data reduction and Don Vandenberg gave essential support. We also thank Tsevi Mazeh for reminding us that dynamical instability imposes maximum periods for planetary companions to binary stars.

This research was supported in part by grants from the Natural Sciences and Engineering Research Council of Canada to Gordon Walker, Don Vandenberg, and Bruce Campbell.

REFERENCES

Basri, G., and G. W. Marcy 1995. A surprise at the bottom of the main sequence: Rapid rotation and no Hα emission *Astrophys. J.* **109,** 762–773.

Boss, A. P. 1995. Proximity of Jupiter-like planets to low-mass stars. *Science* **267,** 360–362.

Burke, B. F. 1992. *TOPS: Toward Other Planetary Systems—A Report by the Solar System Exploration Division.* NASA Publication.

Campbell, B., G. A. H. Walker, and S. Yang 1988. A search for substellar companions to solar-type stars. *Astrophys. J.* **331,** 902–921 (Paper I).

Cochran, W. D., A. P. Hatzes, and T. J. Hancock 1991. Constraints on the companion object to HD 114762. *Astrophys. J.* **380,** L35–L38.

Cochran, W. D., and A. P. Hatzes 1993. McDonald Observatory Planetary search: A high precision stellar radial velocity survey for other planetary systems. In *Planets Around Pulsars* (J. A. Philips, S. E. Thorsett, and S. R. Kulkarni, Eds.), pp. 267–274.

Donnison, J. R., and D. F. Mikulskis 1992. Three-body orbital stability criteria for circular orbits. *Mon. Not. R. Astron. Soc.* **254,** 21–26.

Gatewood, G. D. 1987. The multichannel astrometric photometer and atmospheric limitations in the measurement of relative positions. *Astrophys. J.* **94,** 213–224.

Gray, D. F. 1982. The temperature dependence of rotation and turbulence in giant stars. *Astrophys. J.* **262,** 682–699.

Hatzes, A. P., and W. D. Cochran 1993. Long-period radial velocity variations in three K giants. *Astrophys. J.* **413,** 339–348.

Hershey, J. L. 1977. Parallaxes, mass ratios, and masses for six visual binaries. *Astrophys. J.* **82,** 179–181.

Hoffleit, D., and W. Warren 1991. *The Bright Star Catalogue,* 5th ed. On-line version in Brotzmann, L. E., and Gessner, S. E., *The Astronomical Data Center CD-ROM Selected Astronomical Catalogs,* Vol. 1, Doc. STX-T-1-5002-009-91, NASA, Goddard Space Flight Center (ST Systems Corp.).

Irwin, A. W., B. Campbell, C. L. Morbey, G. A. H. Walker, and S. Yang 1989. Long-period radial-velocity variations of Arcturus. *Publ. Astron. Soc. Pac.* **101,** 147–159.

Irwin, A. W., S. Yang, and G. A. H. Walker 1992a. A precise radial-velocity determination of the orbit of χ^1 Orionis. *Publ. Astron. Soc. Pac.* **104,** 101–105.

IRWIN, A. W., J. M. FLETCHER, S. L. S. YANG, G. A. H. WALKER, AND C. GOODENOUGH 1992b. The orbit and mass of Procyon. *Publ. Astron. Soc. Pac.* **104,** 489–499.

IRWIN, A. W., S. YANG, AND G. A. H. WALKER 1995. The three-dimensional orbit of 36 Ophiuchi AB and constraints on the maximum companion mass. *Publ. Astron. Soc. Pac.* Submitted for publication.

ISAACMAN, R., AND C. SAGAN 1977. Computer simulations of planetary accretion dynamics: sensitivity to initial conditions. *Icarus* **31,** 510–533.

LAGAGE, P. O., AND E. PANTIN 1994. Dust depletion in the inner disk of β Pictoris as a possible indicator of planets. *Nature* **369,** 628–630.

LARSON, A. M., A. W. IRWIN, S. L. S. YANG, C. GOODENOUGH, G. A. H. WALKER, A. WALKER, AND D. A. BOHLENDER 1993a. A Ca II λ8662 index of chromospheric activity: the case of 61 Cygni A. *Publ. Astron. Soc. Pac.* **105,** 332–336.

LARSON, A. M., A. W. IRWIN, S. L. S. YANG, C. GOODENOUGH, G. A. H. WALKER, A. WALKER, AND D. A. BOHLENDER 1993b. A low-amplitude periodicity in the radial velocity and chromospheric emission of β Gemininorum. *Publ. Astron. Soc. Pac.* **105,** 825–831.

LATHAM, D. W., T. MAZEH, R. P. STEFANIK, M. MAYOR, AND G. BURKI 1989. The unseen companion of HD114762: A probable brown dwarf. *Nature,* **339,** 38–40.

MARCY, G. W., AND K. J. BENITZ 1989. A search for sub-stellar companions to low-mass stars. *Astrophys. J.* **344,** 441–453.

MARCY, G. W., AND R. P. BUTLER 1992a. Precision radial velocities with an iodine absorption cell. *Publ. Astron. Soc. Pac.* **104,** 270–277.

MARCY, G. W., AND R. P. BUTLER 1992b. Precision radial velocities using an iodine absorption cell. In *Seeking Other Planetary Systems: The Role of Stellar Radial Velocity Measurements* (D. W. Latham, Ed.), p. 66. Harvard–Smithsonian Center for Astrophysics.

MCMILLAN, R. S., T. L. MOORE, M. L. PERRY, AND P. H. SMITH 1994. Long, accurate time series measurements of radial velocities of stars. *Astrophys. Space Sci.* **212,** 271–280.

MURDOCH, K. A., J. B. HEARNSHAW, AND M. CLARK 1993. A search for substellar companions to southern solar-type stars. *Astrophys. J.* **413,** 349–363.

PRESS, W. H., B. P. FLANNERY, S. A. TEUKOLSKY, AND W. T. VETTERLING 1986. *Numerical Recipes.* Cambridge Univ. Press, Cambridge.

VAN ALTENA, W. F., J. T. LEE, AND D. HOFFLEIT 1991. *The General Catalogue of Trigonometric Parallaxes, A Preliminary Version.* Online version in Brotzmann, L. E., and Gessner, S. E., *The Astronomical Data Center CD-ROM Selected Astronomical Catalogs,* Vol. 1, Doc. STX-T-1-5002-009-91, NASA, Goddard Space Flight Center (ST Systems Corp.).

WALKER, A. R. 1993. *Searching for Planets.* M.Sc. thesis, University of British Columbia.

WALKER, G. A. H., R. JOHNSON, AND S. YANG 1985. Low(est) noise reticon detection systems. In *Advances in Electronics and Electron Physics* (B. L. Morgan, Ed.), Vol. 64A, pp. 213–221. Academic Press, London.

WALKER, G. A. H., S. YANG, B. CAMPBELL, AND A. W. IRWIN 1989. Yellow giants: A new class of radial-velocity variable? *Astrophys. J.* **343,** L21–24.

WALKER, G. A. H., D. A. BOHLENDER, A. R. WALKER, A. W. IRWIN, S. L. S. YANG, AND A. LARSON 1992. γ Cephei: Rotation or planetary companion? *Astrophys. J.* **396,** L91–94.

WALKER, G. A. H., R. JOHNSON, D. RICHARDSON, B. CAMPBELL, A. W. IRWIN, S. YANG 1990. Cross talk in 1872 reticon diode arrays. *Publ. Astron. Soc. Pac.* **102,** 1418–1419.

WOLSZCZAN, A., AND D. A. FRAIL 1992. A planetary system around the millisecond pulsar PSR1257+12. *Nature* **355,** 145–147.

WOLSZCZAN, A. 1994. Confirmation of Earth-mass planets orbiting the millisecond pulsar PSR B1257+12. *Science* **264,** 538–542.

WORLEY, C. W., AND W. D. HEINTZ 1983. *Fourth Catalog of Orbits of Visual Binary Stars.* U.S. Naval Observatory.